Matching the *B*-meson quasidistribution amplitude in the RI/MOM scheme

Ji Xu[*] and Xi-Ruo Zhang[†]

School of Physics and Microelectronics, Zhengzhou University, Zhengzhou, Henan 450001, China

(Received 28 September 2022; accepted 16 November 2022; published 20 December 2022)

Within the framework of large-momentum effective theory, the light-cone distribution amplitude (LCDA) of the B meson in heavy-quark effective theory can be extracted from lattice calculations of the quasidistribution amplitude through the hard-collinear factorization formula. This quasiquantity can be renormalized in a regularization-independent momentum subtraction (RI/MOM) scheme. In this work, we derive the matching coefficient which connects the renormalized quasidistribution amplitude in the RI/MOM scheme and the standard LCDA in the $\overline{\text{MS}}$ scheme at one-loop accuracy. Our numerical analysis verifies the feasibility of the RI/MOM scheme for renormalizing the B-meson quasidistribution amplitude. These results will be crucial for exploring the partonic structure of heavy-quark hadrons.

DOI: 10.1103/PhysRevD.106.114019

I. INTRODUCTION

B-meson light-cone distribution amplitudes (LCDAs) in heavy-quark effective theory (HQET) are the indispensable ingredients for establishing QCD factorization theorems of exclusive B-meson decay amplitudes and for experimental data analysis [1–5]. Defined as the light-cone matrix elements of the nonlocal HQET quark-gluon operators, they describe the nonperturbative strong interaction dynamics of the B-meson system. Although there has been much progress in perturbative calculations concerning B-meson decays in recent years [6–16], our limited knowledge of B-meson LCDAs has become the major stumbling block for precision predictions of the B-meson decay observables. Therefore, currently, a significant task in B physics is improving the accuracy of B-meson LCDAs.

Despite its importance, calculating LCDAs from the first principles of QCD has been a challenge. Model-independent properties of the leading-twist B-meson LCDA $\phi_B^+(\omega,\mu)$ and its first inverse moment $\lambda_B^{-1}(\mu)$ have received considerable attention lately [17–21]. By contrast, nonperturbative determinations of $\phi_B^+(\omega,\mu)$ have been mainly performed in the framework of QCD sum rules or the Dyson-Schwinger equation (DSE) [22,23], whereas both theories have their own drawbacks. In the former, the light-cone separation between the effective heavy-quark field and the light-antiquark field needs to be sufficiently small to guarantee the validity of the local operator product expansion for the HQET correlation function under discussion. In the latter, the DSEs are essentially equations of motion corresponding to the Green's function whose solution requires accurate knowledge of the B-meson wave function. Therefore, it is evident that determining the momentum dependence of B-meson LCDAs with model-independent techniques is of top priority in B physics. Being nonperturbative in nature, LCDAs intrinsically contain low-energy degrees of freedom and thus cannot be evaluated in perturbation theory.

Nonperturbative methods such as lattice QCD offer an alternative way out. Based on first principles, lattice field theory uses the QCD Lagrangian to simulate the strong interaction using Markov chain Monte Carlo methods. In the heavy-quark sector, the relatively large mass of the bottom quark ($m_b \sim 5$ GeV) makes it rather difficult to perform conventional lattice simulations since practical limitations usually cannot permit the use of a sufficiently small lattice spacing a to properly control discretization errors, which necessitates the use of effective field theories such as HQET and nonrelativistic QCD approaches to lattice calculations of the properties of hadrons containing heavy quarks [24,25]. Thanks to long-term efforts from the community, a complete and practical method is known to nonperturbatively renormalize the HQET and match it to QCD in lattice gauge field theory [26–30]. The encouraging results already obtained with the lattice HQET technique bring us confidence for performing the numerical simulation of the leading-twist B-meson LCDA $\phi_B^+(\omega,\mu)$. However, the dependence of the LCDA correlator on the light-cone coordinate makes it essentially unfeasible to directly calculate it on the lattice, which is constructed in Euclidean space with imaginary time.

[*]xuji_phy@zzu.edu.cn
[†]ZXRxiruo@163.com

A promising approach to circumvent this problem was proposed under the name of large-momentum effective theory (LaMET) [31,32]. The essential strategy of this novel proposal resides in the construction of a time-independent quasiquantity which, on the one hand, can be readily computed on a Euclidean lattice and, on the other hand, approaches the original hadronic distribution amplitude on the light cone under a Lorentz boost. The encouraging results obtained in the frame of LaMET indicate that this formalism allows for a bright future to systematically compute a wide range of "parton observables" with the demanding computational resources and the tremendous development of new techniques and algorithms [33–63]. In view of the significance of B-meson LCDAs and the validity of LaMET, more attentions should be devoted to determining B-meson LCDAs in the frame of LaMET, and there have been some preliminary researches [64–66].

Based on LaMET, the procedure of calculating the B-meson LCDA from lattice QCD can be divided into three steps: 1) lattice simulation on the B-meson quasidistribution amplitude; 2. renormalize the quasidistribution amplitude in a specific scheme; 3. match the renormalized quasidistribution amplitude to the LCDA which is usually renormalized in the $\overline{\text{MS}}$ scheme. In this paper, we focus on the second and third steps. With increasing computational resources, the renormalization process will be a key factor to improve the precision of the B-meson quasidistribution amplitude. The authors of Ref. [64] constructed the quasidistribution amplitude $\varphi_B^+(\xi,\mu)$ and renormalized it in the $\overline{\text{MS}}$ scheme. One of the standard methods to renormalize operators in lattice QCD is the regularization-independent momentum subtraction (RI/MOM) scheme which essentially belongs to momentum subtraction schemes in quantum field theory. As a nonperturbative method, it has proven to be practical in the frame of LaMET and gained great popularity in recent years [67–70] (see Refs. [71–74] for other practical approaches). The multiplicative renormalizability of the constructed quasi-HQET operator to all orders in perturbation theory has been demonstrated, which enables a nonperturbative renormalization such as the RI/MOM scheme. This is a crucial step in the application of extracting the B-meson LCDA in lattice simulations. After being renormalized in the RI/MOM scheme, the B-meson quasidistribution amplitude can be matched to the usual B-meson LCDA through the factorization formula. A perturbative matching coefficient appearing in the formula that converts the B-meson quasidistribution amplitude in the RI/MOM scheme to the B-meson LCDA in the $\overline{\text{MS}}$ scheme is not available yet. One of the main motives of this paper is to calculate this coefficient at one-loop accuracy.

Our work is an extension of a series of previous works. The B-meson quasidistribution amplitude $\varphi_B^+(\xi,\mu)$ renormalized in the RI/MOM scheme and the perturbative matching coefficient entering the hard-collinear factorization formula are presented. Since the renormalized matrix elements in the RI/MOM scheme are independent of UV-regularization choices, we carry out this matching calculation with dimensional regularization for convenience. These results will be crucial to exploring the partonic structure of heavy-quark hadrons in the static limit.

The rest of this paper is organized as follows. In Sec. II the leading-twist (twist-2) LCDA and quasi-DA as well as the RI/MOM scheme are briefly reviewed. In Sec. III we present the factorization formula, followed by the calculation of the renormalized quasidistribution amplitude and the derived matching coefficient. In Sec. IV we analyze these results and give perspectives for lattice calculations; a numerical comparison between the B-meson quasidistribution amplitude obtained in the RI/MOM scheme and a modeled B-meson LCDA is presented. We conclude in Sec. V. A few more details about the calculation of the renormalized quasidistribution amplitude are included in the Appendix.

II. B-MESON (QUASI)DISTRIBUTION AMPLITUDES AND RI/MOM SCHEME

The momentum-space distribution function of the leading-twist LCDA $\phi_B^+(\omega,\mu)$ can be deduced from the Fourier transformation of its form in coordinate space [22],

$$\phi_B^+(\omega,\mu)=\frac{1}{2\pi}\int_{-\infty}^{+\infty}d\eta e^{i\bar{n}\cdot v\omega\eta}\tilde{\phi}_B^+(\eta-i\epsilon,\mu), \tag{1}$$

where $\bar{n}$ is the light-cone coordinate with $\bar{n}^2=0$, and $\tilde{\phi}_B^+(\eta,\mu)$ is the leading-twist LCDA in coordinate space with the definition

$$\begin{aligned}&i\tilde{f}_B(\mu)m_B\tilde{\phi}_B^+(\eta,\mu)\\&=\langle 0|(\bar{q}W_c)(\eta\bar{n})\bar{\not{n}}\gamma_5(W_c^\dagger h_v)(0)|\bar{B}(v)\rangle.\end{aligned} \tag{2}$$

The soft light-cone Wilson line is given by $W_c(\eta\bar{n})=\mathrm{P}\{\mathrm{Exp}[ig_s\int_{-\infty}^{\eta}dx\bar{n}\cdot A(x\bar{n})]\}$ and $\tilde{f}_B(\mu)$ is the static decay constant of the B meson [75].

We employ the following definition of the B-meson quasidistribution amplitude:

$$i\tilde{f}_B(\tilde{\mu})m_B\varphi_B^+(\xi,\tilde{\mu}) = \int_{-\infty}^{+\infty}\frac{d\tau}{2\pi}e^{in_z\cdot v\xi\tau}\langle 0|(\bar{q}W_c)(\tau n_z)\not{n}_z\gamma_5(W_c^\dagger h_v)(0)|\bar{B}(v)\rangle. \tag{3}$$

Here $\tilde{\mu}$ is a renormalization scale for the quasidistribution amplitude whose definition depends on the renormalization scheme we choose. One can see that $\varphi_B^+(\xi,\tilde{\mu})$ is constructed from the spatial correlation function of two collinear (effective) quark fields with $n_z=(0,0,0,1)$, and we work in a Lorentz-boosted frame of the B meson in which $\bar{n}\cdot v \gg n\cdot v$ and set $v_{\perp\mu}=0$. Unlike the B-meson LCDA defined in Eq. (1), which is invariant under a boost along the z direction, the quasidistribution amplitude changes dynamically under such a boost, which is encoded in its nontrivial dependence on the heavy-quark velocity v.

It is of vital importance to show that the nonlocal matrix element in Eq. (3) will renormalize multiplicatively to all orders in perturbation theory when applying the lattice regularization scheme since this feature will facilitate the lattice QCD simulation substantially. The authors of Ref. [64] demonstrated this multiplicative renormalizability, which enables the RI/MOM scheme to be utilized in the B-meson quasidistribution amplitude $\varphi_B^+(\xi,\tilde{\mu})$. Following the strategy in Refs. [49,50], the RI/MOM renormalization factor $Z_{\rm OM}$ is determined nonperturbatively on the lattice by imposing the condition that the quantum corrections of the correlator in an off-shell quark state vanish at the scales $k^2=-\mu_R^2$ and $k^z=k_R^z$,

$$Z_{\rm OM}^{-1}(\tau,k_R^z,\mu_R,\Lambda)\langle 0|(\bar{q}W_c)(\tau n_z)\not{n}_z\gamma_5(W_c^\dagger h_v)(0)|b\bar{q}(k)\rangle|_{\substack{k^2=-\mu_R^2\\k^z=k_R^z}} = \langle 0|(\bar{q}W_c)(\tau n_z)\not{n}_z\gamma_5(W_c^\dagger h_v)(0)|b\bar{q}(k_R)\rangle|_{\rm tree}, \tag{4}$$

where μ_R is the renormalization scale. For convenience, hereafter we simply denote $\{\tilde{\mu}\}=\{k^2=-\mu_R^2,k^z=k_R^z\}$. It should be stressed that the renormalization condition is applied to the matrix element, not the quasidistribution itself. In order to get the renormalized quasidistribution, one needs to Fourier transform this matrix element afterwards. The operator in Eq. (4) is not $O(4)$ covariant; therefore, in addition to μ_R, one needs another scale parameter k_R^z to pin down the renormalization condition. Λ denotes the UV cutoff, in the case of dimensional regularization $\Lambda=1/\epsilon$.

We denote the bare correlator for the B meson on the lattice as

$$\tilde{h}_B(\tau,k^z,1/\epsilon) = \langle 0|(\bar{q}_s W_c)(\tau n_z)\not{n}_z\gamma_5(W_c^\dagger h_v)(0)|b\bar{q}(k)\rangle, \tag{5}$$

which is renormalized as

$$\tilde{h}_R(\tau,k^z,\{\tilde{\mu}\}) = Z_{\rm OM}^{-1}(\tau,\{\tilde{\mu}\},1/\epsilon)\tilde{h}_B(\tau,k^z,1/\epsilon). \tag{6}$$

One advantage of the RI/MOM scheme is that, although the bare matrix element and the renormalization factor $Z_{\rm OM}$ depend on the choice of regularization scheme, the renormalized matrix element does not. Besides, the logarithmic UV divergence related to the self-energy of the quark and the linear divergence arising from the self-energy of the Wilson line have been delicately discussed in Ref. [42]. All of the UV cutoff dependence cancels out in Eq. (6) due to the multiplicative renormalizability of the quasidistribution amplitude.

Afterwards, by Fourier transforming the renormalized matrix element $\tilde{h}_R(\tau,k^z,\{\tilde{\mu}\})$ to momentum space, one can work out the RI/MOM matching coefficient. This issue will be elaborately discussed in the next section.

III. MATCHING BETWEEN QUASIDISTRIBUTION AMPLITUDE AND LIGHT-CONE DISTRIBUTION AMPLITUDE

We now proceed to determine the perturbative matching coefficient that converts the renormalized B-meson quasidistribution amplitude in the RI/MOM scheme to the renormalized B-meson LCDA in the $\overline{\rm MS}$ scheme. Following the construction in Ref. [64], the hard-collinear factorization formula is

$$\varphi_B^+(\xi,\tilde{\mu}) = \int_0^\infty d\omega H(\xi,\omega,n_z\cdot v,\mu,\{\tilde{\mu}\})\phi_B^+(\omega,\mu) + \mathcal{O}\left(\frac{\Lambda_{\rm QCD}}{n_z\cdot v\xi}\right). \tag{7}$$

For convenience, hereafter we subsequently denote $n_z\cdot v$ as v^z. The matching coefficient H denotes the difference in the UV behavior of the quasiquantity and the light-cone one (one can resort to the recent reviews in Refs. [55,56] for more details). Thanks to the asymptotic freedom, this difference can be calculated using perturbation theory in QCD, which makes it possible to extract light-cone parton physics from quasiquantities. Notably, the matching coefficient H depends on the choice of the renormalization scheme for the quasidistribution amplitude.

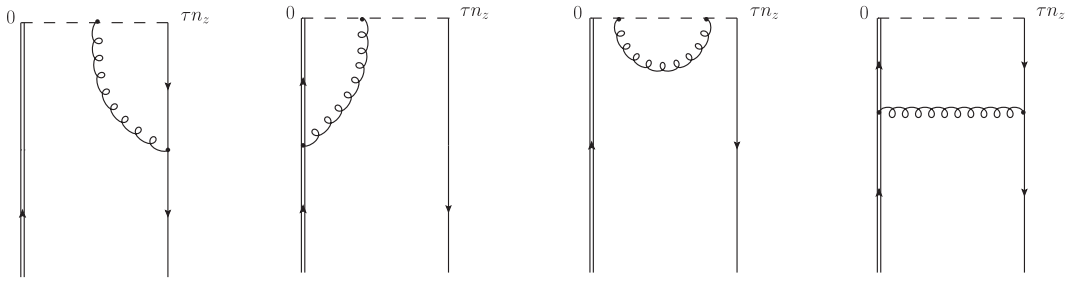

FIG. 1. One-loop corrections to the quasidistribution amplitude $\varphi_B^+(\xi,\mu)$: the effective HQET bottom quark is represented by the double line, and the spacelike Wilson line is indicated by the dashed line.

To determine the matching coefficient at the one-loop level, we replace the B-meson state with a heavy b quark plus an off-shell light-quark state in Eqs. (2) and (3). Then, the matrix elements with the quark state as the initial state can be calculated in perturbation theory. We carry out the calculation using the off-shellness of the light quark as an IR regulator and dimensional regularization with $d = 4 - 2\epsilon$ as the UV regulator.

The one-loop corrections to the quasidistribution amplitude of $\varphi_B^+(\xi,\tilde{\mu})$ are shown in Fig. 1. The result at tree level is $\varphi_B^{+(0)}(\xi) = \delta(\xi - \tilde{k})$, where $\tilde{k} \equiv k^z/v^z$. We denote the result for the bare quasidistribution amplitude at one loop as $\varphi_{B,\mathrm{bare}}^{+(1)}(\xi,\mu)$, which was calculated in Ref. [64]:

$$\varphi_{B,\mathrm{bare}}^{+(1)}(\xi,\mu) = \frac{\alpha_s C_F}{4\pi}\begin{cases} \left(\frac{1}{\tilde{k}(\xi-\tilde{k})}\left(-\tilde{k} + 2\xi\ln\frac{-\xi}{\tilde{k}-\xi}\right)\right) + \left[\frac{2}{\tilde{k}-\xi}\right]_\oplus + \left[\frac{1}{\xi-\tilde{k}}\left(\frac{1}{\epsilon} - \ln 4 + \ln\frac{\mu^2}{v^{z2}(\tilde{k}-\xi)^2}\right)\right]_\oplus & (\xi < 0) \\ \frac{1}{\tilde{k}(\xi-\tilde{k})}\left(2\xi - \tilde{k} - 2\ln\frac{4\tilde{k}^2 v^{z2}}{-k^2}\right) + \left[\frac{2}{\tilde{k}-\xi}\right]_\oplus + \left[\frac{1}{\xi-\tilde{k}}\left(\frac{1}{\epsilon} - \ln 4 + \ln\frac{\mu^2}{v^{z2}(\tilde{k}-\xi)^2}\right)\right]_\oplus & (0 < \xi < \tilde{k}) \\ \frac{1}{\tilde{k}(\xi-\tilde{k})}\left(\tilde{k} - 2\xi\ln\frac{\xi}{\xi-\tilde{k}}\right) + \left[\frac{2}{\xi-\tilde{k}}\right]_\oplus + \left[\left(\frac{1}{\epsilon} + \ln 4 + 2\ln v^{z2} + \ln\frac{\mu^2}{v^{z2}(\xi-\tilde{k})^2}\right)\right]_\oplus & (\xi > \tilde{k}) \end{cases}$$
$$+ \frac{\alpha_s C_F}{4\pi} f(a)\delta(\xi - \tilde{k}). \tag{8}$$

Here we assign $v^\mu = (v^0, 0, 0, v^z)$, with $v^z \gg 1$. Applying the default power-counting scheme, one can readily identify that the hard correction from the one-loop box diagram in Fig. 1(d) is power suppressed. Recall that we have used the off-shellness of the light quark $-k^2$ as an IR regulator; this logarithmic IR singularity is identical for both quasidistribution amplitude and LCDA, leaving the matching coefficient H independent of $-k^2$, as it should be.

The plus distribution is defined by (with $a > 1$)

$$\{F(\xi,\omega)\}_\oplus = F(\xi,\omega) - \delta(\xi-\omega)\int_0^{a\xi} dt F(\xi,t). \tag{9}$$

The subtraction-scheme-dependent term in Eq. (8),

$$\begin{aligned} f(a) = {} & -\frac{1}{\epsilon}(1 + \ln(4(a-1)v^{z2})) - 2 - \frac{\pi^2}{3} + 4(\ln 2)^2 + \ln\frac{128}{a-1} + (\ln a - 1)^2 \\ & + 2\ln a + \ln v^{z2}(3 + 2\ln 4 + \ln v^{z2}) + \ln(4v^{z2})(3\ln(a-1) - 2\ln a) \\ & + \mathrm{HPL}[\{-,+\},-1] - 2\ln\frac{-k^2}{\tilde{k}^2}\left(1 + \ln\frac{a-1}{a}\right) + \ln\frac{\xi^2}{\mu^2}(1 + \ln(4(a-1)v^{z2})), \end{aligned} \tag{10}$$

will compensate the same scheme dependence of the newly introduced plus distribution for the convolution of the hard function H with a smooth test function. An advantage of introducing the above-mentioned plus function is that it allows to implement both the ultraviolet and infrared subtractions for the perturbative matching procedure simultaneously.

Having the bare result in hand, we next discuss the RI/MOM renormalization of $\varphi_B^+(\xi,\tilde{\mu})$. The renormalized correlator $\tilde{h}_R(\tau,k^z,\{\tilde{\mu}\})$ was already given in Eq. (6), which must be Fourier transformed into ξ space to obtain the distribution $\tilde{\mathcal{F}}(\xi,k^z,\{\tilde{\mu}\})$:

$$\tilde{\mathcal{F}}(\xi,k^z,\{\tilde{\mu}\})=\int\frac{d\tau}{2\pi}e^{iv^z\xi\tau}\tilde{h}_R(\tau,k^z,\{\tilde{\mu}\}). \tag{11}$$

$\tilde{\mathcal{V}}(k^z,\{\tilde{\mu}\})$ is the local correspondence of $\tilde{\mathcal{F}}(\xi,k^z,\{\tilde{\mu}\})$, which is given by $\tilde{h}_R$ at $\tau=0$,

$$\tilde{\mathcal{V}}(k^z,\{\tilde{\mu}\})=\tilde{h}_R(\tau=0,k^z,\{\tilde{\mu}\}). \tag{12}$$

With $\tilde{\mathcal{F}}(\xi,k^z,\{\tilde{\mu}\})$ and $\tilde{\mathcal{V}}(k^z,\{\tilde{\mu}\})$ calculated on the lattice, the B-meson quasidistribution amplitude can be obtained as

$$\varphi_B^+(\xi,\tilde{\mu})=v^z\int\frac{d\tau}{2\pi}e^{iv^z\xi\tau}\frac{\tilde{h}_R(\tau,k^z,\{\tilde{\mu}\})}{\tilde{h}_R(\tau=0,k^z,\{\tilde{\mu}\})}. \tag{13}$$

The calculation procedure of the renormalization factor Z_{OM} is similar to the previous one in Ref. [64] but a bit more complicated, since the Feynman diagrams in Fig. 1 are calculated at a specific scale $\{\tilde{\mu}\}$. We then proceed to derive the expression for the renormalized quasidistribution amplitude $\varphi_B^+(\xi,\tilde{\mu})$ from Eq. (13). Taking advantage of Eq. (6), we have

$$\varphi_B^+(\xi,\tilde{\mu})=v^z\int\frac{d\tau}{2\pi}e^{iv^z\xi\tau}\frac{Z_{\mathrm{OM}}^{-1}(\tau,\{\tilde{\mu}\},1/\epsilon)}{Z_{\mathrm{OM}}^{-1}(0,\{\tilde{\mu}\},1/\epsilon)}\frac{\tilde{h}_B(\tau,k^z,1/\epsilon)}{\tilde{h}_B(0,k^z,1/\epsilon)}. \tag{14}$$

The renormalization constant is determined by the renormalization condition in Eq. (4),

$$\frac{Z_{\mathrm{OM}}^{-1}(\tau,\{\tilde{\mu}\},1/\epsilon)}{Z_{\mathrm{OM}}^{-1}(0,\{\tilde{\mu}\},1/\epsilon)}\frac{\tilde{h}_B(\tau,\{\tilde{\mu}\},1/\epsilon)}{\tilde{h}_B(0,\{\tilde{\mu}\},1/\epsilon)}=\left.\frac{\tilde{h}_B(\tau,\{\tilde{\mu}\},1/\epsilon)}{\tilde{h}_B(0,\{\tilde{\mu}\},1/\epsilon)}\right|_{\mathrm{tree}},$$
$$=e^{-ik_R^z\tau}, \tag{15}$$

in which

$$\frac{\tilde{h}_B(\tau,\{\tilde{\mu}\},1/\epsilon)}{\tilde{h}_B(0,\{\tilde{\mu}\},1/\epsilon)}=\int d\xi' e^{-i\tau v^z\xi'}\varphi_{B,\mathrm{CT}}^+(\xi',\{\tilde{\mu}\}). \tag{16}$$

Here $\varphi_{B,\mathrm{CT}}^+$ is the additive counterterm contribution of the quasidistribution amplitude, as will be clearly seen subsequently. Substitute Eq. (16) into Eq. (15), one immediately obtains the ratio of the nonlocal and local renormalization constants at one loop,

$$\left(\frac{Z_{\mathrm{OM}}^{-1}(\tau,\{\tilde{\mu}\},1/\epsilon)}{Z_{\mathrm{OM}}^{-1}(0,\{\tilde{\mu}\},1/\epsilon)}\right)^{(1)}$$
$$=-\int d\xi' e^{-i\tau(v^z\xi'-k_R^z)}\varphi_{B,\mathrm{CT}}^{+(1)}(\xi',\{\tilde{\mu}\}), \tag{17}$$

as well as $\left(\frac{Z_{\mathrm{OM}}^{-1}(\tau,\{\tilde{\mu}\})}{Z_{\mathrm{OM}}^{-1}(0,\{\tilde{\mu}\})}\right)^{(0)}=1$ at tree level.

Finally, the renormalized quasidistribution amplitude in Eq. (14) can be expanded at one-loop order,

$$\begin{aligned}\varphi_B^{+(1)}(\xi,\tilde{\mu})&=v^z\int\frac{d\tau}{2\pi}e^{iv^z\xi\tau}\left\{\left(\frac{Z_{\mathrm{OM}}^{-1}(\tau,\{\tilde{\mu}\},1/\epsilon)}{Z_{\mathrm{OM}}^{-1}(0,\{\tilde{\mu}\},1/\epsilon)}\right)^{(1)}\left(\frac{\tilde{h}(\tau,k^z)}{\tilde{h}(0,k^z)}\right)^{(0)}+\left(\frac{Z_{\mathrm{OM}}^{-1}(\tau,\{\tilde{\mu}\})}{Z_{\mathrm{OM}}^{-1}(0,\{\tilde{\mu}\})}\right)^{(0)}\left(\frac{\tilde{h}_B(\tau,k^z,1/\epsilon)}{\tilde{h}_B(0,k^z,1/\epsilon)}\right)^{(1)}\right\}\\&=-v^z\int\frac{d\tau}{2\pi}e^{iv^z\xi\tau}\int d\xi' e^{-i\tau(v^z\xi'-k_R^z)}\varphi_{B,\mathrm{CT}}^{+(1)}(\xi',\{\tilde{\mu}\})e^{-ik^z\tau}+\varphi_{B,\mathrm{bare}}^{+(1)}(\xi,k^z)\\&=\varphi_{B,\mathrm{bare}}^{+(1)}(\xi,k^z)-\varphi_{B,\mathrm{CT}}^{+(1)}(\xi+\tilde{k}_R-\tilde{k},r_R).\end{aligned} \tag{18}$$

Here $\tilde{k}_R\equiv k_R^z/v^z$ and we define the dimensionless ratio

$$r_R\equiv\frac{\mu_R^2}{k_R^{z2}}. \tag{19}$$

It is worth stressing the difference between r_R and $\rho\equiv-k^2/k^{z2}$. As indicated, we keep $-k^2$ small as the IR regulator, i.e., $\rho\ll1$. Thus, we can identify the logarithmic IR divergences by Taylor expanding in ρ, making the calculation much more convenient. However, the renormalization scale μ_R is not necessarily small, which makes a Taylor expansion in r_R unfeasible when calculating the renormalized quasidistribution amplitude, i.e., calculating the counterterm of the bare quasidistribution amplitude. More pertinent details on this issue can be found in the Appendix.

Next, we consider the B-meson LCDA $\phi_B^+(\omega,\mu)$ whose IR divergence is regulated by the same light-quark off-shellness $-k^2$. With the definition in Eq. (1), one can get the renormalized $\phi_B^+(\omega,\mu)$ at one loop in the $\overline{\mathrm{MS}}$ scheme:

$$\phi_B^{+(1)}(\omega,\mu)=\frac{\alpha_s C_F}{2\pi}\begin{cases}0 & (\omega<0)\\ \left[-\frac{\omega}{(\omega-\tilde{k})\tilde{k}}\ln\frac{\mu^2\tilde{k}^2}{\omega(\tilde{k}-\omega)(-k^2)}\right]_\oplus & (0<\omega<\tilde{k})\\ \left[\frac{1}{\omega-\tilde{k}}\ln\frac{\mu^2}{(\omega-\tilde{k})^2}\right]_\oplus & (\omega>\tilde{k})\end{cases}$$
$$-\frac{\alpha_s C_F}{2\pi}\left[-2+\frac{5\pi^2}{24}+\frac{1}{2}(\ln(a-1))^2+(\ln a)^2+\mathrm{Li}_2(1-a)\right.$$
$$\left.+(\ln a-1)\ln\left(-\frac{\mu^2}{k^2}\right)-\ln(a-1)\ln\left(-\frac{a\mu^2}{k^2}\right)+\left(\ln\frac{\omega}{\mu}\right)^2\right]\delta(\omega-\tilde{k}). \tag{20}$$

The results shown in Eqs. (20) and (8) do not contain the contribution of the box diagram since the collinear contribution to the bare quasidistribution amplitude in the box diagram is precisely reproduced by the corresponding diagram for the B-meson LCDA at one loop, i.e., in the unphysical region ($\xi<0$) the contribution of the box diagram to the quasiquantity is suppressed by $1/v_z^2$, and in the physical region ($\omega>0$) the contributions to both the quasiquantity and LCDA are exactly the same. As for the counterterm in the box diagram for the quasidistribution amplitude in the RI/MOM scheme, as long as we work in the region $v^{z2}\xi\gg 1/r_R$ the contribution can be disregarded. In fact, it has also been demonstrated that the box diagram does not contribute in the pseudodistribution approach either [76].

Considering the hard-collinear factorization formula in Eq. (7), the matching coefficient H is then determined by the difference between the momentum-space quasidistribution amplitude and the LCDA. We expand $\varphi_B^+(\xi,\tilde{\mu}),\phi_B^+(\omega,\mu)$, and $H(\xi,\omega,v^z,\mu,\{\tilde{\mu}\})$ in series of α_s^n up to the one-loop level:

$$\begin{aligned}\varphi_B^+(\xi,\tilde{\mu})&=\delta(\xi-\tilde{k})+\varphi_B^{+(1)}(\xi,\tilde{\mu})+\mathcal{O}(\alpha^2),\\ \phi_B^+(\omega,\mu)&=\delta(\omega-\tilde{k})+\phi_B^{+(1)}(\omega,\mu)+\mathcal{O}(\alpha^2),\\ H(\xi,\omega,v^z,\mu,\{\tilde{\mu}\})&=\delta(\xi-\omega)+H^{(1)}(\xi,\omega,v^z,\mu,\{\tilde{\mu}\})\\ &\quad+\mathcal{O}(\alpha^2).\end{aligned} \tag{21}$$

Substituting the expressions above into Eq. (7),

$$H^{(1)}(\xi,\omega,v^z,\mu,\{\tilde{\mu}\})|_{\omega\to\tilde{k}}=\varphi_B^{+(1)}(\xi,\tilde{\mu})-\phi_B^{+(1)}(\omega,\mu)|_{\omega\to\xi}. \tag{22}$$

The renormalized $\varphi_B^{+(1)}(\xi,\tilde{\mu})$ and $\phi_B^{+(1)}(\omega,\mu)$ have already been calculated, and therefore the matching coefficient can be derived from Eq. (22),

$$H(\xi,\omega,v^z,\mu,\{\tilde{\mu}\})=\delta(\xi-\omega)+g_1(\xi,\omega,\mu)-g_2(\xi,\omega,\{\tilde{\mu}\})+\frac{\alpha_s C_F}{4\pi}\ln v^z\left(3+4\ln\frac{a-1}{a}\right)\delta(\xi-\omega), \tag{23}$$

where

$$g_1(\xi,\omega,\mu)=\frac{\alpha_s C_F}{4\pi}\begin{cases}\frac{1}{\omega(\omega-\xi)}\left(\omega-2\xi\ln\frac{-\xi}{\omega-\xi}\right) & (\xi<0)\\ \left[\frac{1}{\omega(\omega-\xi)}\left(\omega-2\xi+2\xi\ln\frac{4v^{z2}\xi(\omega-\xi)}{\mu^2}\right)\right]_\oplus & (0<\xi<\omega)\\ \left[\frac{1}{\omega(\omega-\xi)}\left(-\omega+2\omega\ln\frac{\mu^2}{(\xi-\omega)^2}+2\xi\ln\frac{\xi}{\xi-\omega}\right)\right]_\oplus & (\xi>\omega)\end{cases} \tag{24}$$

and

$$g_2(\xi,\omega,\{\tilde{\mu}\}) = \frac{\alpha_s C_F}{4\pi}\begin{cases} -\frac{1}{\omega-\xi} & (\xi < \omega - \tilde{k}_R) \\ \left[\frac{1}{2k_R^z\sqrt{1-r_R}(\omega-\xi)}\left(-2\sqrt{1-r_R}(k_R^z + 2v^z(\xi-\omega))\right.\right. & \\ \left.\left. -(4v^z(\xi-\omega) - k_R^z(r_R-4))\ln\frac{2-2\sqrt{1-r_R}-r_R}{r_R}\right)\right]_\oplus & (\omega - \tilde{k}_R < \xi < \omega) \\ \left[\frac{1}{\omega-\xi}\right]_\oplus & (\xi > \omega). \end{cases} \tag{25}$$

As expected, H does not depend on the IR regulator $-k^2$ since the logarithmic IR singularities cancel between the quasidistribution amplitude and the LCDA. The $\mathcal{O}(1/v^{z2})$ contributions to the matching coefficient H are dropped, and the v^z expansion is subtle and thus should be treated carefully and systematically. One can tell that the expression for H is more complicated than that in Ref. [64] where the quasidistribution amplitude was renormalized in the $\overline{\text{MS}}$ scheme; this is natural since the renormalization condition in the RI/MOM scheme has introduced new momentum scales $\{\tilde{\mu}\}$. In Sec. IV we will make a comparison between these two matching coefficients.

IV. PERSPECTIVES FOR LATTICE CALCULATIONS

We discuss the perspectives for lattice calculations based on numerical analysis. An important step in obtaining the B-meson LCDA in HQET based upon LaMET is to perform the lattice simulation of the quasidistribution amplitude $\varphi_B^+(\xi,\tilde{\mu})$ in the moving B-meson frame with $v^z \gg 1$. To this end, it will be instructive to study how the matching coefficient in Eq. (23) changes the LCDA, which is helpful for understanding the characteristic feature of $\varphi_B^+(\xi,\tilde{\mu})$. We start with a well-known phenomenological model of $\phi_B^+(\omega,\mu)$ motivated by the HQET sum rule calculation [1],

$$\phi_B^+(\omega,\mu = 1.5\text{ GeV}) = \frac{\omega}{\omega_0^2}e^{-\omega/\omega_0}, \tag{26}$$

where the reference value of the logarithmic inverse moment $\omega_0 = 350$ MeV is taken for illustrative purposes. With the expression for $\phi_B^+(\omega,\mu)$ above and the factorization formula in Eq. (7), we can depict the shape of the quasidistribution amplitude $\varphi_B^+(\xi,\tilde{\mu})$. For our study, we set the default values $k_R^z = 2$ GeV, $\mu = 1.5$ GeV, and $r_R = 2$. The factorization formula in Eq. (7) requires a large v^z in order to suppress the $\mathcal{O}(1/v^{z2})$ corrections; here, we take $v^z = 10$. Figure 2 shows comparisons between the RI/MOM quasidistribution amplitude (blue dashed line), the $\overline{\text{MS}}$ quasidistribution amplitude (orange dashed line), and the modeled LCDA of the B meson (red solid line). One can see that both the RI/MOM and $\overline{\text{MS}}$ quasidistribution amplitudes are close to the B-meson LCDA, and the radiative tail at large and negative momentum ξ that develops in the $\overline{\text{MS}}$ quasidistribution amplitude does not emerge in the RI/MOM quasidistribution amplitude, which is encouraging on account of the convergence of perturbation theory in the RI/MOM scheme. In addition, in contrast to the quasiparton distribution function in Ref. [42], no peaks arise in the momentum region $\xi \le 0$. Next, we consider the dependence of the RI/MOM quasidistribution amplitude on r_R and k_R^z. We fix $k_R^z = 2$ GeV, $\mu = 1.5$ GeV, and $v^z = 10$ and vary the parameter $r_R = \{1.5, 4, 12\}$ in the upper panel of Fig. 3. One can tell that the quasidistribution amplitude is pretty sensitive to the variation of r_R. It seems that with larger r_R, the quasidistribution amplitude moves away from LCDA. In the lower panel of Fig. 3 we vary $k_R^z = \{1, 2, 4\}$ GeV with fixed values of $r_R = 2, \mu = 1.5$ GeV, and $v^z = 10$.

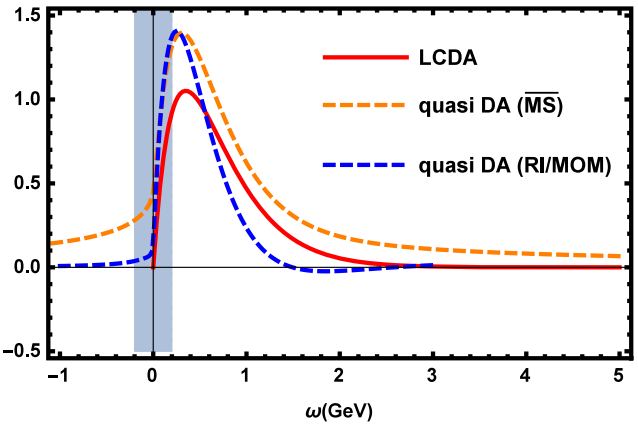

FIG. 2. Shapes of the B-meson quasidistribution amplitude $\varphi_B^+(\xi = \omega, k_R^z = 2.0\text{ GeV}, r_R = 2)$ in HQET obtained from the hard-collinear factorization theorem in Eq. (7) and from the nonperturbative model of $\phi_B^+(\omega,\mu = 1.5\text{ GeV})$ presented in Eq. (26). The red solid line represents the nonperturbative model of ϕ_B^+, whereas the corresponding quasidistribution amplitudes φ_B^+ normalized in the $\overline{\text{MS}}$ and RI/MOM schemes are represented by the orange dashed and blue dashed lines, respectively. The shadow region of $|\omega| \le 200$ MeV is excluded due to the inapplicability of the hard-collinear factorization formula for $|v^z\omega| \le 2.0$ GeV.

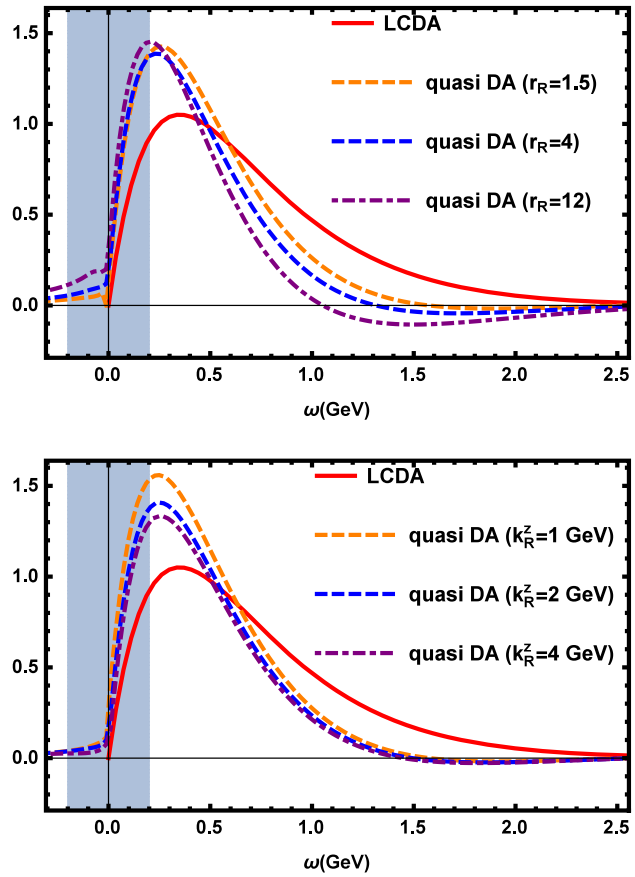

FIG. 3. Comparisons between the LCDA and the quasidistribution amplitude obtained at different r_R's (upper panel) and k_R^z's (lower panel).

Finally, we discuss the dependence on the heavy-quark velocity v^z. We hold $k_R^z = 2$ GeV, $\mu = 1.5$ GeV, and $r_R = 2$ and vary $v^z = \{3, 10, 20\}$ in Fig. 4. The differences between quasidistribution amplitudes depicted with different v^z values decreases rapidly as ω increases. When $\omega > 0.8$ the three lines almost merge into one, which was also observed in the study of the quasiparton distribution function using different P^z values [42], suggesting that the RI/MOM scheme is a promising approach with favorable convergence at large ω.

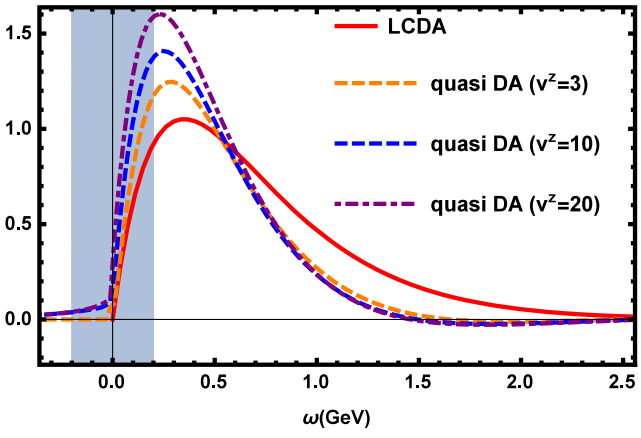

FIG. 4. Comparisons between the LCDA and the quasidistribution amplitude obtained at $v^z = 3$ (orange dashed), $v^z = 10$ (blue dashed), and $v^z = 20$ (purple dashed).

It should be stressed here that the current lattice HQET studies mainly focus on the spectroscopy, decay constants, and transition form factors of heavy mesons. For the case of nonlocal heavy-light currents, the situation could be more complicated. On the one hand, we should construct a fully nonperturbative renormalization program for the currents (this is what this work is trying to partially address). On the other hand, quantifying the size of discretization errors beyond the naive power-counting analysis is also called for, especially when we need a rather large momentum for the heavy meson. This is an issue that should be studied further in the future.

In addition, with increasing computational resources, one can further decrease the lattice spacing to $a \leq 0.044$ fm, at which point even bottom quarks could be simulated with the same action as up/down quarks, in principle, although this would be relatively computationally expensive. Thus, we can pursue an alternative determination of the B-meson distribution amplitude $\phi_B^+(\omega, \mu)$ from the numerical simulation of the following Euclidean quantity directly in QCD:

$$if_B m_B \psi_B^+(x,\mu) = \int_{-\infty}^{+\infty} \frac{d\tau}{2\pi} e^{in_z\cdot p x\tau} \langle 0|(\bar{q}W_c)(\tau n_z)\not{n}_z\gamma_5(W_c^\dagger b)(0)|\bar{B}(p)\rangle. \tag{27}$$

From the perspective of continuum QCD, the newly introduced distribution amplitude $\psi_B^+(x,\mu)$ can be further matched onto the Euclidean HQET quantity $\varphi_B^+(\xi,\mu)$ by integrating out the short-distance fluctuations at the heavy-quark mass scale, in analogy to the hard-collinear factorization formula obtained in Refs. [12,77].

In conclusion, the numerical analysis in this section indicates that the RI/MOM scheme is suitable for renormalizing the B-meson quasidistribution amplitude. The derived one-loop matching coefficient yields only a relatively small effect on the modeled B-meson LCDA, which provides more confidence about extracting the B-meson LCDA perturbatively and model independently in the future. It should be stressed here that our major objective is to explore the opportunity of accessing the light-cone dynamics of the B-meson leading-twist distribution amplitude by simulating the RI/MOM quasidistribution amplitude on the lattice. This is a rather preliminary attempt, and the numerical simulations of such quasidistribution amplitudes are still at an exploratory stage, even for the ones suitable for the determination of the light-meson distribution amplitude. Improved methodologies to control

both the statistical errors and systematic uncertainties are called for, as well as further development of new algorithms and computing techniques on the lattice (see Refs. [55,56,78,79] for details on lattice calculations). We would also like to remind the reader that a hybrid renormalization procedure was recently proposed for the quasiparton distribution function, which utilizes the advantages of the RI/MOM and ratio schemes at short and large distances simultaneously [51]. The study of the feasibility of this renormalization procedure applied to the B-meson quasidistribution amplitude deserves more attention.

V. CONCLUSION

LaMET theory has provided a natural way to calculate parton distributions in an interval of momentum scales, similar to extracting parton distributions from experimental data at finite energies. Within the framework of LaMET, we derived the matching coefficient which connects the renormalized quasidistribution amplitude in the RI/MOM scheme and the standard LCDA in the $\overline{\text{MS}}$ scheme. Our numerical analysis indicates that the one-loop matching has a nice UV convergence and reasonable magnitude as a perturbative correction, which shows that the theoretical uncertainty caused by perturbative matching is controllable, thus making the RI/MOM scheme feasible in lattice applications. We believe that our result has the potential to considerably improve the convenience and accuracy of extracting the B-meson LCDA from quasiquantities, and hence to promote the development of a first-principles determination of the highly desired B-meson LCDA, which is undoubtedly of the highest importance for exploring the delicate flavor structure of the Standard Model and beyond at the LHCb and Belle II experiments.

To further increase the accuracy of our results, one can study the yet unavailable higher-order perturbative corrections to the short-distance matching coefficient and construct the subleading-power factorization formula for the quasidistribution amplitude, which we leave for future works.

ACKNOWLEDGMENTS

We thank Wei Wang for careful reading of the manuscript and suggestions. We are also grateful to Shuai Zhao for inspiring discussions and valuable comments on the renormalization process of the B-meson quasidistribution amplitude. J. X. and X.-R. Z are supported by the National Natural Science Foundation of China under Grants No. 12105247 and 12047545, and by the China Postdoctoral Science Foundation under Grant No. 2021M702957.

APPENDIX: RENORMALIZATION OF B-MESON QUASIDISTRIBUTION AMPLITUDE

First, consider the amplitude of the heavy-quark sail diagram in Fig. 1(b),

$$\varphi^{+(b)}_{B,\text{bare}}(\xi,\mu) = ig_s^2 C_F \tilde{\mu}^{2\epsilon} v^z \int \frac{d^d q}{(2\pi)^d} \frac{1}{q^z} \frac{1}{q^2} \frac{1}{v\cdot q} \times (\delta(\xi-\tilde{k}+q^z)-\delta(\xi-\tilde{k})). \tag{A1}$$

Here the delta functions $\delta(\xi-\tilde{k}+q^z)$ and $\delta(\xi-\tilde{k})$ in the parentheses in Eq. (A1) come from the Fourier transformation with respect to the variable τ in the "real" and "virtual" diagrams, respectively. Notably, all of the k dependence comes from the delta function, while the other part of the integrand is independent of k^z and $\rho \equiv -k^2/k^{z2}$, indicating that the corresponding counterterm $\varphi^{+(b)}_{B,\text{CT}}(\xi+\tilde{k}_R-\tilde{k},r_R)$ in Eq. (18) remains unchanged when the RI/MOM renormalization condition is imposed at the specific scale $\{\tilde{\mu}\}$,

$$\varphi^{+(b)}_{B,\text{CT}}(\xi+\tilde{k}_R-\tilde{k},r_R) = ig_s^2 C_F \tilde{\mu}^{2\epsilon} v^z \int \frac{d^d q}{(2\pi)^d} \frac{1}{q^z} \frac{1}{q^2} \frac{1}{v\cdot q} \times (\delta(\xi-\tilde{k}+q^z)-\delta(\xi-\tilde{k})). \tag{A2}$$

Therefore, the contribution of the heavy-quark sail diagram cancels out after renormalization. This feature which appears in the RI/MOM B-meson quasidistribution amplitude considerably simplifies our calculation and facilitates a relatively small effect of the final one-loop matching coefficient. A similar cancelation also appears in the Wilson line self-energy diagram in Fig. 1(c),

$$\varphi^{+(c)}_{B,\text{bare}}(\xi,\mu) = -ig_s^2 C_F \tilde{\mu}^{2\epsilon} \int \frac{d^d q}{(2\pi)^d} \frac{1}{q^2} \frac{1}{q^{z2}} \times (\delta(\xi-\tilde{k}+q^z)-\delta(\xi-\tilde{k})). \tag{A3}$$

Once again, except for the delta function, the integrand in Eq. (A3) is independent of k^z and ρ, indicating that the contributions of the bare term and counterterm cancel out after RI/MOM renormalization.

As for the box diagram in Fig. 1(d), the result for the bare quasidistribution amplitude reads

$$\varphi^{+(d)}_{B,\text{bare}}(\xi,\mu) = \frac{\alpha_s C_F}{2\pi}\left\{ -\frac{\xi}{\tilde{k}(\tilde{k}-\xi)} \ln\frac{\xi}{\xi-\tilde{k}}\theta(\xi-\tilde{k}) + \frac{\xi}{\tilde{k}(\tilde{k}-\xi)} \ln\frac{-k^2}{\tilde{k}^2}\theta(0<\xi<\tilde{k}) + (0)\theta(\xi<0)\right\} + \mathcal{O}(1/v^{z2}). \tag{A4}$$

It is worth noting that the contribution to the bare quasidistribution amplitude in the box diagram in the physical region [$\theta(\xi-\tilde{k})$ and $\theta(0<\xi<\tilde{k})$] is exactly the same as the corresponding box diagram for the B-meson LCDA, and the contribution in the unphysical region ($\xi<0$) is suppressed by $1/v_z^2$ (the contribution of

the B-meson LCDA in the unphysical region is 0). Besides, the box diagram does not introduce any UV divergence and therefore, despite of its intricate form, the corresponding counterterm for the quasidistribution amplitude provides only finite terms of $O(1/v^{z2})$. To summarize the above, the box diagram does not contribute to the matching coefficient within $\mathcal{O}(1/v^{z0})$ accuracy. In fact, it was already shown in Refs. [64,66] that the box diagram does not contribute in either the LaMET or pseudodistribution approach.

Finally, we consider the light-quark sail diagram in Fig. 1(a). The expression for the bare quasidistribution amplitude is

$$\varphi^{+(a)}_{B,\mathrm{bare}}(\xi,\mu) = -ig_s^2 C_F(\tilde{\mu})^{2\epsilon}\int\frac{d^dq}{(2\pi)^d}\frac{1}{q^z}\frac{1}{q^2}\frac{1}{(q+k)^2}(k^z(\rho-2)-q^z-q^t\sqrt{1-\rho})(\delta(\xi-\tilde{k}-q^z)-\delta(\xi-\tilde{k})). \tag{A5}$$

We have utilized a projection operator to deal with the Dirac matrix $\bar{v}(k)\Gamma u_v(p_b) \to \mathrm{Tr}[\frac{1+\not{v}}{2}M_b\not{v}\gamma_5\not{k}\Gamma]$. In addition to the delta function, the other part of the integrand in Eq. (A5) has a k dependence. The result for the bare amplitude was already calculated in Ref. [64].

As for the counterterm in the RI/MOM scheme, it is determined by setting $k^2 = -\mu_R^2$ and $k^z = k_R^z$,

$$\varphi^{+(a)}_{B,\mathrm{CT}}(\xi+\tilde{k}_R-\tilde{k},r_R) = -ig_s^2 C_F(\tilde{\mu})^{2\epsilon}\int\frac{d^dq}{(2\pi)^d}\frac{1}{q^z}\frac{1}{q^2}\frac{1}{(q+k_R)^2}(k_R^z(r_R-2)-q^z-q^t\sqrt{1-r_R})(\delta(\xi-\tilde{k}-q^z)-\delta(\xi-\tilde{k})). \tag{A6}$$

The r_R is not necessarily small, which makes a Taylor expansion in r_R unfeasible in our calculations. After introducing the Feynman parameter α and integrating the $d-1$ dimensions of the integral momentum q, we have

$$\begin{aligned}\varphi^{+(a)}_{B,\mathrm{CT}}(\xi+\tilde{k}_R-\tilde{k},r_R) = &-\frac{2\alpha_s C_F}{8\pi^{\frac{3}{2}}}\int_0^1 d\alpha\int_{-\infty}^{+\infty}dq^z\frac{e^{\gamma_E\epsilon}\mu^{2\epsilon}(q^z+k_R^z(2+\alpha(r_R-1)-r_R))\Gamma(\frac{1}{2}+\epsilon)}{q^z(q^{z2}+2k_R^zq^z\alpha+k_R^{z2}\alpha(\alpha+r_R-\alpha r_R))^{\frac{1}{2}+\epsilon}}\\ &\times(\delta(\xi-\tilde{k}-q^z)-\delta(\xi-\tilde{k})).\end{aligned} \tag{A7}$$

Subsequently, we integrate out α and q^z and get the result for this counterterm, which will be incorporated into the final result for the renormalized quasidistribution amplitude in Eq. (A8) below.

With all of the results shown above at one loop, the renormalized quasidistribution amplitude can be written as

$$\varphi_B^+(\xi,\tilde{\mu}) = \delta(\xi-\tilde{k})+h_1(\xi,\tilde{k})-h_2(\xi,\{\tilde{\mu}\})+\frac{\alpha_s C_F}{4\pi}\ln v^z\left(3+4\ln\frac{a-1}{a}\right)\delta(\xi-\tilde{k}), \tag{A8}$$

where

$$h_1(\xi,\tilde{k}) = \frac{\alpha_s C_F}{4\pi}\begin{cases}\frac{1}{\tilde{k}(\xi-\tilde{k})}\left(-\tilde{k}+2\xi\ln\frac{-\xi}{\tilde{k}-\xi}\right) & (\xi<0)\\ \left[\frac{1}{\tilde{k}(\xi-\tilde{k})}\left(2\xi-\tilde{k}-2\xi\ln\frac{4\tilde{k}^2v^{z2}}{-k^2}\right)\right]_\oplus & (0<\xi<\tilde{k})\\ \left[\frac{1}{\tilde{k}(\xi-\tilde{k})}\left(\tilde{k}-2\xi\ln\frac{\xi}{\xi-\tilde{k}}\right)\right]_\oplus & (\xi>\tilde{k})\end{cases} \tag{A9}$$

and

$$h_2(\xi,\{\tilde{\mu}\}) = \frac{\alpha_s C_F}{4\pi}\begin{cases} \frac{1}{\xi-\tilde{k}} & (\xi < \tilde{k}-\tilde{k}_R) \\ \left[\frac{1}{2k_R^z\sqrt{1-r_R}(\tilde{k}-\xi)}\left(-2\sqrt{1-r_R}(k_R^z+2v^z(\xi-\tilde{k}))\right.\right. & \\ \left.\left.+(k_R^z(r_R-4)+4v^z(\tilde{k}-\xi))\ln\frac{2-2\sqrt{1-r_R}-r_R}{r_R}\right)\right]_\oplus & (\tilde{k}-\tilde{k}_R < \xi < \tilde{k}) \\ \left[-\frac{1}{\xi-\tilde{k}}\right]_\oplus & (\xi > \tilde{k}). \end{cases} \tag{A10}$$

Inserting the renormalized quasidistribution amplitude $\varphi_B^+(\xi,\tilde{\mu})$ in Eq. (A8) and the renormalized LCDA $\phi_B^+(\omega,\mu)$ in Eq. (20) into Eq. (22), we get the expected matching coefficient in Eq. (23).

[1] A. G. Grozin and M. Neubert, Phys. Rev. D **55**, 272 (1997).
[2] M. Beneke, G. Buchalla, M. Neubert, and C. T. Sachrajda, Phys. Rev. Lett. **83**, 1914 (1999).
[3] M. Beneke and T. Feldmann, Nucl. Phys. **B592**, 3 (2001).
[4] M. Beneke, T. Feldmann, and D. Seidel, Nucl. Phys. **B612**, 25 (2001).
[5] T. Becher, R. J. Hill, and M. Neubert, Phys. Rev. D **72**, 094017 (2005).
[6] Y. M. Wang, Nucl. Part. Phys. Proc. **285–286**, 75 (2017).
[7] Y. M. Wang, J. High Energy Phys. 09 (2016) 159.
[8] T. Feldmann, B. O. Lange, and Y. M. Wang, Phys. Rev. D **89**, 114001 (2014).
[9] G. Bell, T. Feldmann, Y. M. Wang, and M. W. Y. Yip, J. High Energy Phys. 11 (2013) 191.
[10] A. M. Galda, M. Neubert, and X. Wang, J. High Energy Phys. 07 (2022) 148.
[11] H. Deng, J. Gao, L. Y. Li, C. D. Lü, Y. L. Shen, and C. X. Yu, Phys. Rev. D **103**, 076004 (2021).
[12] S. Zhao, Phys. Rev. D **101**, 071503 (2020).
[13] D. H. Yao, X. Liu, Z. T. Zou, Y. Li, and Z. J. Xiao, arXiv:2202.10010.
[14] J. Chai, S. Cheng, Y. h. Ju, D. C. Yan, C. D. Lü, and Z. J. Xiao, arXiv:2207.04190.
[15] S. Cheng and Z. J. Xiao, Front. Phys. **16**, 24201 (2021).
[16] J. Chai, S. Cheng, and A. J. Ma, Phys. Rev. D **105**, 033003 (2022).
[17] B. O. Lange and M. Neubert, Phys. Rev. Lett. **91**, 102001 (2003).
[18] V. M. Braun, Y. Ji, and A. N. Manashov, Phys. Rev. D **100**, 014023 (2019).
[19] S. J. Lee and M. Neubert, Phys. Rev. D **72**, 094028 (2005).
[20] Y. M. Wang and Y. L. Shen, J. High Energy Phys. 05 (2018) 184.
[21] M. Beneke, V. M. Braun, Y. Ji, and Y. B. Wei, J. High Energy Phys. 07 (2018) 154.
[22] V. M. Braun, D. Y. Ivanov, and G. P. Korchemsky, Phys. Rev. D **69**, 034014 (2004).
[23] F. Gao, L. Chang, Y. X. Liu, C. D. Roberts, and S. M. Schmidt, Phys. Rev. D **90**, 014011 (2014).
[24] E. Eichten and B. R. Hill, Phys. Lett. B **240**, 193 (1990).
[25] G. P. Lepage, L. Magnea, C. Nakhleh, U. Magnea, and K. Hornbostel, Phys. Rev. D **46**, 4052 (1992).
[26] N. H. Christ, M. Li, and H. W. Lin, Phys. Rev. D **76**, 074505 (2007).
[27] B. Blossier, M. D. Morte, P. Fritzsch, N. Garron, J. Heitger, H. Simma, R. Sommer, and N. Tantalo (ALPHA Collaboration), J. High Energy Phys. 09 (2012) 132.
[28] M. D. Morte, S. Dooling, J. Heitger, D. Hesse, and H. Simma (ALPHA Collaboration), J. High Energy Phys. 05 (2014) 060.
[29] N. Brambilla, J. Komijani, A. S. Kronfeld, and A. Vairo (TUMQCD Collaboration), Phys. Rev. D **97**, 034503 (2018).
[30] F. Bahr, D. Banerjee, F. Bernardoni, A. Joseph, M. Koren, H. Simma, and R. Sommer (ALPHA Collaboration), Phys. Lett. B **757**, 473 (2016).
[31] X. Ji, Phys. Rev. Lett. **110**, 262002 (2013).
[32] X. Ji, Sci. China Phys. Mech. Astron. **57**, 1407 (2014).
[33] X. Ji, A. Schäfer, X. Xiong, and J. H. Zhang, Phys. Rev. D **92**, 014039 (2015).
[34] X. Xiong and J. H. Zhang, Phys. Rev. D **92**, 054037 (2015).
[35] H. n. Li, Phys. Rev. D **94**, 074036 (2016).
[36] T. Ishikawa, Y. Q. Ma, J. W. Qiu, and S. Yoshida, arXiv:1609.02018.
[37] C. Monahan and K. Orginos, J. High Energy Phys. 03 (2017) 116.
[38] M. Constantinou and H. Panagopoulos, Phys. Rev. D **96**, 054506 (2017).
[39] X. Ji, J. H. Zhang, and Y. Zhao, Phys. Rev. Lett. **120**, 112001 (2018).
[40] Y. Jia, S. Liang, L. Li, and X. Xiong, J. High Energy Phys. 11 (2017) 151.
[41] W. Wang, S. Zhao, and R. Zhu, Eur. Phys. J. C **78**, 147 (2018).
[42] I. W. Stewart and Y. Zhao, Phys. Rev. D **97**, 054512 (2018).
[43] W. Wang and S. Zhao, J. High Energy Phys. 05 (2018) 142.
[44] J. Xu, Q. A. Zhang, and S. Zhao, Phys. Rev. D **97**, 114026 (2018).
[45] S. S. Xu, L. Chang, C. D. Roberts, and H. S. Zong, Phys. Rev. D **97**, 094014 (2018).

[46] A. V. Radyushkin, Phys. Lett. B **788**, 380 (2019).
[47] J. H. Zhang, X. Ji, A. Schäfer, W. Wang, and S. Zhao, Phys. Rev. Lett. **122**, 142001 (2019).
[48] Z. Y. Li, Y. Q. Ma, and J. W. Qiu, Phys. Rev. Lett. **122**, 062002 (2019).
[49] Y. S. Liu, W. Wang, J. Xu, Q. A. Zhang, J. H. Zhang, S. Zhao, and Y. Zhao, Phys. Rev. D **100**, 034006 (2019).
[50] Y. S. Liu, W. Wang, J. Xu, Q. A. Zhang, S. Zhao, and Y. Zhao, Phys. Rev. D **99**, 094036 (2019).
[51] X. Ji, Y. Liu, A. Schäfer, W. Wang, Y. B. Yang, J. H. Zhang, and Y. Zhao, Nucl. Phys. **B964**, 115311 (2021).
[52] J. Hua *et al.* (Lattice Parton Collaboration), Phys. Rev. Lett. **129**, 132001 (2022).
[53] J. Hua *et al.* (Lattice Parton (LPC) Collaboration), Proc. Sci., LATTICE2021 (**2022**) 322.
[54] J. Hua, M.-H. Chu, P. Sun, W. Wang, J. Xu, Y.-B. Yang, J.-H. Zhang, and Q.-A. Zhang (Lattice Parton Collaboration), Phys. Rev. Lett. **127**, 062002 (2021).
[55] X. Ji, Y. S. Liu, Y. Liu, J. H. Zhang, and Y. Zhao, Rev. Mod. Phys. **93**, 035005 (2021).
[56] K. Cichy and M. Constantinou, Adv. High Energy Phys. **2019**, 3036904 (2019).
[57] M. Bhat, W. Chomicki, K. Cichy, M. Constantinou, J. R. Green, and A. Scapellato, Phys. Rev. D **106**, 054504 (2022).
[58] C. Egerer, R. G. Edwards, C. Kallidonis, K. Orginos, A. V. Radyushkin, D. G. Richards, E. Romero, and S. Zafeiropoulos (HadStruc Collaboration), J. High Energy Phys. 11 (2021) 148.
[59] C. Alexandrou, M. Constantinou, K. Hadjiyiannakou, K. Jansen, and F. Manigrasso, Phys. Rev. Lett. **126**, 102003 (2021).
[60] C. Alexandrou, K. Cichy, M. Constantinou, K. Hadjiyiannakou, K. Jansen, A. Scapellato, and F. Steffens, Phys. Rev. Lett. **125**, 262001 (2020).
[61] S. Bhattacharya, K. Cichy, M. Constantinou, A. Metz, A. Scapellato, and F. Steffens, Phys. Rev. D **102**, 034005 (2020).
[62] Y. Su, J. Holligan, X. Ji, F. Yao, J. H. Zhang, and R. Zhang, arXiv:2209.01236.
[63] R. Zhang, J.-W. Chen, L. Jin, H.-W. Lin, A. Schäfer, P. Sun, Y.-B. Yang, J.-H. Zhang, and Y. Zhao (LP3 Collaboration), Nucl. Phys. **B939**, 429 (2019).
[64] W. Wang, Y. M. Wang, J. Xu, and S. Zhao, Phys. Rev. D **102**, 011502 (2020).
[65] H. Kawamura and K. Tanaka, Proc. Sci., RADCOR2017 (**2018**) 076.
[66] J. Xu, X. R. Zhang, and S. Zhao, Phys. Rev. D **106**, L011503 (2022).
[67] C. Alexandrou, K. Cichy, M. Constantinou, K. Hadjiyiannakou, K. Jansen, H. Panagopoulos, and F. Steffens, Nucl. Phys. **B923**, 394 (2017).
[68] J. W. Chen, T. Ishikawa, L. Jin, H. W. Lin, Y. B. Yang, J. H. Zhang, and Y. Zhao, Phys. Rev. D **97**, 014505 (2018).
[69] H.-W. Lin, J.-W. Chen, T. Ishikawa, and J.-H. Zhang (LP3 Collaboration), Phys. Rev. D **98**, 054504 (2018).
[70] J. Green, K. Jansen, and F. Steffens, Phys. Rev. Lett. **121**, 022004 (2018).
[71] A. V. Radyushkin, Phys. Rev. D **96**, 034025 (2017).
[72] K. Orginos, A. Radyushkin, J. Karpie, and S. Zafeiropoulos, Phys. Rev. D **96**, 094503 (2017).
[73] V. M. Braun, A. Vladimirov, and J. H. Zhang, Phys. Rev. D **99**, 014013 (2019).
[74] Z. Y. Li, Y. Q. Ma, and J. W. Qiu, Phys. Rev. Lett. **126**, 072001 (2021).
[75] M. Beneke and D. Yang, Nucl. Phys. **B736**, 34 (2006).
[76] S. Zhao and A. V. Radyushkin, Phys. Rev. D **103**, 054022 (2021).
[77] S. Ishaq, Y. Jia, X. Xiong, and D. S. Yang, Phys. Rev. Lett. **125**, 132001 (2020).
[78] C. Alexandrou, K. Cichy, M. Constantinou, K. Hadjiyiannakou, K. Jansen, A. Scapellato, and F. Steffens, Phys. Rev. D **99**, 114504 (2019).
[79] R. Zhang, Z. Fan, R. Li, H. W. Lin, and B. Yoon, Phys. Rev. D **101**, 034516 (2020).